VOLUME 40 NUMBER 8

ACCOUNTS of CHEMICAL RESEARCH®

AUGUST 2007

Registered in U.S. Patent and Trademark Office; Copyright 2007 by the American Chemical Society

Interface-Mediated Growth of Monodispersed Nanostructures

XUN WANG, QING PENG, AND YADONG LI*

Department of Chemistry, Tsinghua University, Beijing 100084, China

Received December 7, 2006

ABSTRACT

This Account focuses on the recent development of interface-mediated growth of monodispersed nanostructures in our laboratory. By rationally tuning the chemical reactions at various gas–liquid, solid–solid, liquid–liquid, and liquid–solid–solution interfaces, we could readily synthesize nanostructures such as hollow microspheres, core–shell nanoparticles, and monodispersed nanocrystals. These advances in interface-mediated synthesis could lead to progress in the development of nanocrystal crystallography and encourage some more unique and exciting research and applications to nanoscience and nanotechnology.

1. Introduction

Interfaces are formed between two different phases with common boundaries. The boundary region is characteristic of forces acting on it by the particles involved. As a result of interfacial interactions, atoms at the interfaces are more prone to react with the surrounding species and to produce many useful properties which have attracted scientists' interest.[1,2]

Recent progress in the research of low-dimensional nanostructures highlights interfaces as the key factors for the controlled growth of these novel building blocks.[3–16] The formation of the low-dimensional nanostructures is a process that involves the generation and expansion of interfaces between the target nanosolid and their surrounding bulk vapor, liquid, or solid matter.[3] Since the interface regions have a thickness on the order of several atoms, a dimension comparable to that of the nanostructures, the control over the dynamic process across the interfaces is usually the determining factor for the growth of nanostructures while they might be negligible for bulk materials. Scientists have made great efforts in utilizing the interface regions for guided growth of various nanostructures. In a typical vapor–liquid–solid process to produce one-dimensional (1D) nanowires,[4–8] the sizes of the liquid metal catalyst were kept at several nanometers, which would create a nanoscale gas–liquid and liquid–solid interface. Then the growth of 1D nanostructures can be directed by the introduction of these nanoscale interfaces. Monodispersed colloidal nanocrystals are another distinguished class of nanostructures, whose growth relies heavily on the control of the interface chemistry.[9–13] The colloidal nanocrystals are composite materials with inorganic nanocrystals as the core and the surfactant as the shell.[9] As the main pathway, the inorganic–organic interfaces will determine the transporting behavior of ion and atom species across the nanocrystals and their outer surrounding and thus affect the growth dynamic of nanocrystals.[14,15] To some extent, the main challenge in this promising field is how to engineer these interfaces.

The existence of different types of interfaces in a system depends on the condensed state of matter: gas–liquid, liquid–solid, solid–solid, liquid–liquid (different in polarity), etc.[1,2] If one could achieve a precise control over the interfaces, the crystallization process of a nanostructure could be achieved. In general, careful design of the nanoscale interfaces between different forms of condensed matter would result in a series of novel nanostructures: (1) gas–liquid interfaces can be utilized as the

Xun Wang received his B.S. degree from the Department of Chemical Engineering, Northwest University (China), in 1998 and Ph.D. degree in Chemistry from Tsinghua University in 2004, under the direction of Professor Yadong Li. He joined the faculty of the Department of Chemistry, Tsinghua University, in 2004 and was promoted to associate professor in 2005.

Qing Peng received his B.S. degree in Chemistry from Peking University in 1992 and Ph.D. degree in Chemistry from Tsinghua University in 2003, under the direction of Professor Yadong Li. He joined the faculty of the Department of Chemistry, Tsinghua University, in 2003 and was promoted to associate professor in 2006.

Yadong Li received his B.S. degree in Chemistry from Anhui Normal University in 1986 and Ph.D. degree in Chemistry from the University of Science and Technology of China in 1998, under the direction of Professor Yitai Qian. He joined the faculty of the Department of Chemistry, Tsinghua University, in 1999 as a full professor.

* To whom correspondence should be addressed. E-mail: ydli@tsinghua.edu.cn.

10.1021/ar600007y CCC: $37.00 © 2007 American Chemical Society
Published on Web 05/12/2007

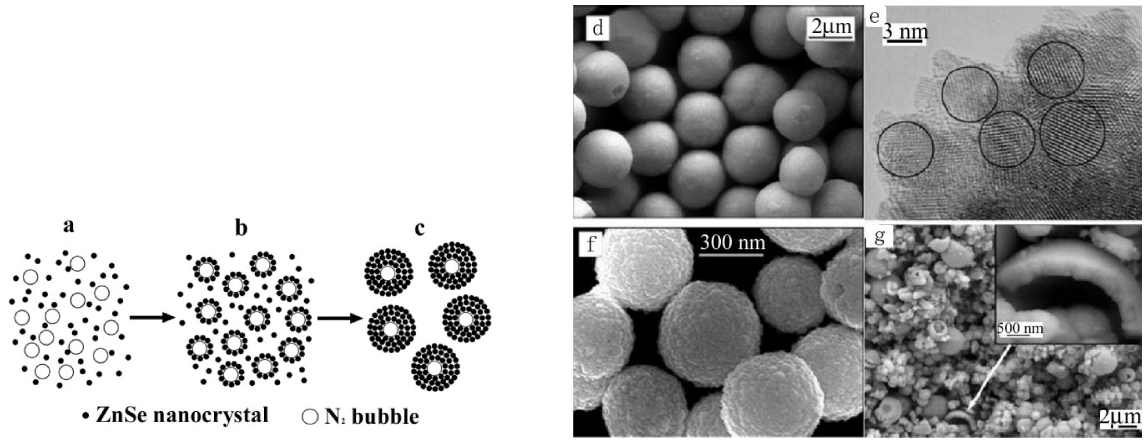

FIGURE 1. (a–c) Schematic representation of the gas–liquid interface condensed mechanism for the formation of ZnSe microspheres. (d) ZnSe microspheres with diameters of 2 μm. (e) HRTEM image of ZnSe microspheres after grinding, which indicates that the microspheres are the aggregation of small nanocrystals with a size of 5–6 nm. (f) ZnSe microspheres with diameters of 300 nm. (g) SEM image of the broken ZnSe microspheres. The inset shows an individual broken shell, which indicates that these microspheres are hollow.

agglomeration center for nanocrystals[17] or the nucleation center for the nanocrystals;[4–8] (2) solid–solid interfaces would generate various core–shell[18–20] or nanotape[21] nanostructures; and (3) organic–inorganic interfaces would generate different nanocomposite materials or monodispersed colloidal nanocrystals.[9–13]

This Account summarizes our recent endeavor in the study on the interface-mediated growth of monodispersed nanocrystals and is organized into three parts. The first part is a review of a gas–liquid interface condensation mechanism for preparing ZnSe hollow microspheres, which then act as active templates for the generation of various semiconductor hollow nanostructures via interface-controlled reactions. The second part summarizes the development of solid–solid interface-controlled growth of a series of metal–carbon core–shell nanostructures and metal oxide hollow spheres. The third part presents our recent progress in the liquid–solid–solution phase transfer and separation process and the positive emulsion method for the growth of monodispersed nanocrystals in general.

2. Gas–Liquid Interface Condensed Mechanism to ZnSe Hollow Microspheres and Their Conversion to Semiconductor Microspheres via Surface-Controlled Reactions

Gas–Liquid Interface Condensed Mechanism to ZnSe Hollow Microspheres. The gases generated in a liquid-phase chemical reaction are usually released as bubbles, which will create numerous gas–liquid interfaces inside the continuous solution phase. Similar to the gas–liquid interfaces in a VLS mechanism,[4–8] the gas–liquid interfaces in continuous solution may serve as the nucleation or agglomeration centers for the nanocrystals. Especially in an aqueous solution system, the surface of the in situ-generated nanocrystals is not protected well with foreign species like surfactants, so they have the tendency to aggregate together to release the high surface energy of the nanocrystals. The formation of the bubbles in the reaction system may enable this agglomeration process to proceed in a controllable way. With the introduction of microbubbles into the reaction system, the agglomeration process may occur around the bubble. This process is apparently thermodynamically favorable. On one hand, the forces on the solvent molecules at the concave interfaces (between the bubbles and the bulk liquid phase) are asymmetric so that these molecules need other species (e.g., nanocrystals) to stabilize. On the other hand, the high surface tension of nanocrystals should be released to reach a stable state. As a result, the in situ-generated nanocrystals tend to move into the interface region. When the concentration of nanocrystals in this region is sufficiently high, the tiny nanocrystals will interact with each other to form hollow microsphere nanostructures with the bubbles as soft physical templates. This process has been named a "gas–liquid interface aggregation mechanism".[17]

This mechanism has been applied to the controlled growth of ZnSe hollow microspheres for the first time. The chemical reaction can be described as follows:

$$2SeO_3^{2-} + 2ZnO_2^{2-} + 3N_2H_4 \rightarrow 2ZnSe + 3N_2\uparrow + 2H_2O + 8OH^- \quad (1)$$

In this reaction, the SeO_3^{2-} ions were reduced first by hydrazine to Se atoms, which were further reduced or disproportionated in the alkaline solution to generate Se^{2-} ions;[22] then these ions reacted with ZnO_2^{2-} to form ZnSe monomers. As illustrated in Figure 1a–c, after the initial nucleation, the monomers would grow into nanocrystals (step a), which had a tendency to aggregate. At the same time, large quantities of microbubbles of N_2 produced in the reaction might serve as the aggregation center (step b). Due to the minimization of interfacial energy, small ZnSe nanocrystals may aggregate around the gas–liquid interface between N_2 and water (step b), and finally, hollow ZnSe microspheres formed (step c).

On the basis of the "gas–liquid interface aggregation mechanism",[17] the size of N_2 bubbles and the concentration and aggregation radius of the ZnSe monomers played important roles in determining the final size of the hollow ZnSe microspheres. The size could be adjusted by controlling the viscosity of the solution, the supply rate of

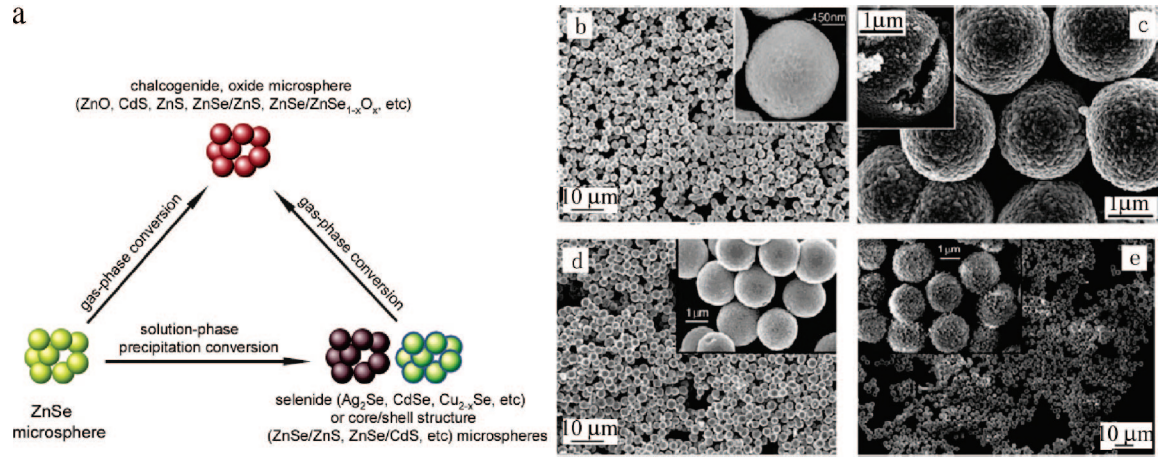

FIGURE 2. (a) Schematic illustration of the chemical conversion method to semiconductor hollow microspheres and their core–shell structures. SEM images of ZnO (b), Ag_2Se (c), $Cu_{2-x}Se$ (d), and CdSe (e) microspheres obtained via the surface-controlled chemical conversion method.

Zn^{2+} ions, and the mobility of the ZnSe monomers. In our experiments, parameters such as the concentration of the raw materials and/or the reaction temperature as well as complexing agents were used to control the supply rate of Zn^{2+} ions. Through competition between complexation and precipitation in solution, different complexing agents could result in different supply rates, and thus, the diameter of the microspheres could be modulated (Figure 1d–g).

The use of gas bubbles generated during the reaction to provide aggregation centers is a novel and effective method for fabricating hollow microspheres. Compared to the other template-synthetic methods, this simple soft-template method will avoid the introduction of impurities and is therefore suitable for modern chemical synthesis. This idea could be extended to other solution systems in which easily aggregated monodispersed nanocrystals are produced during the reaction. The gas bubbles will help these nanocrystals to aggregate to form hollow microspheres.

Conversion of ZnSe Hollow Microspheres into Semiconductor Hollow Microspheres. Unlike inert SiO_2 and polystyrene microspheres, the interior of the ZnSe nanocrystals is more reactive. Furthermore, ZnSe has a relatively large solubility product constant ($K_{sp} = 10^{-29.4}$) compared with those of other metal selenides (or tellurides) (for example, $K_{sp} = 10^{-35.2}$, $10^{-63.7}$, $10^{-48.1}$, $10^{-42.1}$, $10^{-64.5}$, $10^{-31.2}$, and $10^{-32.7}$ for CdSe, Ag_2Se, CuSe, PbSe, HgSe, CoSe, and NiSe, respectively). This indicates that the ZnSe microspheres can act as both reactants to synthesize more stable chalcogenides and oxides and templates to produce structures with a hollow-sphere morphology.[23] On the basis of this concept, a convenient chemical conversion mechanism (Figure 2a) has been established. In this process, liquid–solid and gas–solid interfaces were intentionally introduced into the reaction system. Since ZnSe microspheres were composed of numerous nanocrystals, they exhibited good permeability in solution. Ions and H_2O molecules could therefore move inside the spheres with relative ease, which helped to ensure that the target semiconductor microspheres were pure-phase compounds.

Through a solution-phase precipitation conversion involving the reaction of ZnSe with metal ions, a number of selenide hollow microspheres with lower K_{sp} values could be conveniently obtained at low temperatures (Figure 2c,d). For heavy metal ions such as Ag^+, Cu^{2+}, Pb^{2+}, and Hg^{2+}, whose selenides with K_{sp} have values significantly lower than that of ZnSe, the equilibrium constant (K) value for the conversion reaction is nonetheless large enough. These ions could react with ZnSe at room temperature rapidly, and the corresponding selenide microspheres could easily be obtained by immersing the ZnSe microspheres into solutions with excess metal ions.

However, to obtain microspheres of transition metal selenides whose K_{sp} values are very close to or only a little lower than that of ZnSe (e.g., CdSe, CoSe, and NiSe), high ionic concentrations and additional energy input (by heating to 140 °C) were required to successfully complete the conversion reaction (Figure 2e). By introducing other soluble chalcogen sources into the reaction system, this precipitation conversion method could also be used to synthesize microspheres with core–shell structures. For example, when an appropriate amount of thioacetamide was introduced into the system, ZnSe–ZnS and ZnSe–CdS core–shell microspheres could be prepared.

In addition to solution-phase conversion, gas-phase reactions were also effective for carrying out this chemical conversion method. By reacting the as-prepared selenide microspheres with oxygen or gaseous sulfur at a relatively higher temperature, we could prepare more stable oxide or sulfide (or their composite) microspheres. For example, after ZnSe microspheres were heated in air for 3 h, a ZnO sample was obtained (Figure 2b). With the protection of an argon atmosphere, ZnS and CdS samples were obtained after heating the starting selenide microspheres with sulfur powders at 400 °C for 3 h. From the SEM images, it was clear that the samples retained their spherical morphology.

Following the surface-controlled reactions described above, a series of semiconductor hollow microspheres have been successfully synthesized. These hollow micro-

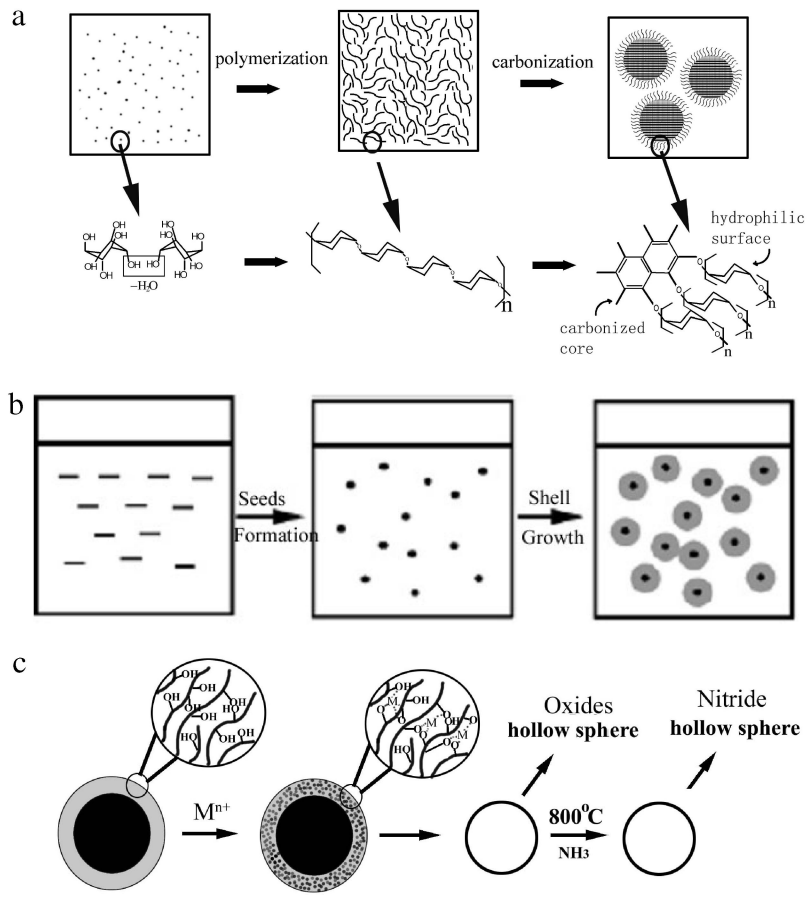

FIGURE 3. (a) Schematic growth model for carbonaceous spheres. (b) Schematic illustration of the formation of Ag@C core–shell structured nanospheres. (c) Schematic mechanism for the formation of GaN hollow spheres using carbon spheres as templates.

spheres may find applications in the fields of delivery vehicle systems, catalysts, etc. Furthermore, these hollow structures might be considered as potential candidates for electrode materials in photochemical solar cells and be expected to exhibit high light collection efficiency and a fast motion of charge carriers due to their hollow and closely packed structures.

3. Solid–Solid Interface-Mediated Formation of Core–Shell Nanostructures and Hollow Spheres

There are many types of solid–solid interfaces which are of interest to chemists and materials scientists.[2] As for the preparations of nanostructures, careful design of solid–solid interfaces may result in core–shell structures,[19,20] nanocomposite materials,[21] etc., in which the different solid regions are separated spatially on a nanometer scale. To control the overgrowth dynamics of one crystalline nanosolid upon another, the epitaxy growth strategy was widely adopted.[2,18–20] In this process, a nanometer-scale layer would be deposited onto the surface of the as-prepared nanocrystals (core or templates) to form the core–shell structures, and the size of the target structures was mainly determined by the size of the core as well as the thickness of the shell. The key to the success of this approach would be how to design the surface properties of initial cores or templates so that they have better compatibility with the shell. Apparently, if the inner or outer surfaces of the initial cores or templates were functionalized in situ, additional surface modification would be avoided, and the subsequent epitaxy growth processes would be desirable as more convenient ways for the controlled growth of core–shell nanostructures or hollow spheres. Carbonaceous microspheres may represent such novel core or template structures.[24–30]

Recently, uniform carbonaceous microspheres have been prepared via the dehydration and aromatization of a glucose solution under hydrothermal conditions (Figure 3a).[24] These carbonaceous microspheres have many important features: (1) tunable and uniform sizes of 150–1500 nm, (2) hydrophilic and reactive surfaces due to the existence of functional groups like OH^-, CHO^-, and COO^- groups, and (3) porous microstructures. The active surface and porous microstructures are interesting with respect to the interface-mediated synthesis of core–shell structures in which the deposition of other species onto the porous and active surface is much easier than onto an inert and dense one. Our experimental results show that these carbonaceous spheres have shown an amazing ability to encapsulate noble metal nanoparticles to form carbon–metal core–shell nanostructures[24–26] or act as new-type active physical templates for the formation of various oxides or nitride hollow microspheres.[27–30]

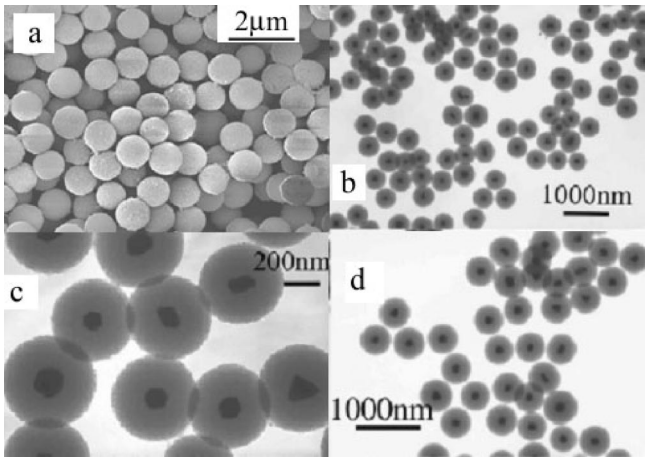

FIGURE 4. (a) Typical SEM image of carbonaceous spheres. (b–d) Ag@C core–shell nanospheres with different sizes.

In these processes, various solid–solid interfaces have been generated intentionally.

One-Step Encapsulation Reaction for Synthesizing Carbon@Ag Core–Shell Nanostructures. The formation of Ag@C core–shell structured nanospheres involved two primary steps (Figure 3b): nucleation of inner silver nanoparticles and consequent epitaxial growth and thickening of the carbonaceous shell on the silver core.[24,25] Initially, both $AgNO_3$ and glucose were dissolved in deionized water which resulted in a clear and homogeneous solution. As the $AgNO_3$ was reduced by glucose, Ag nanoparticles nucleated and exposed the outer reactive surface to catalyze the following carbonization of glucose and led to in situ deposition of carbonaceous products around the Ag nanoparticle surface to form a carbonaceous shell. In this process, the solid–solid interface was created along with the formation of silver nanoparticles, and the interaction between the functional groups in the carbonaceous shell and the surface of the silver core was achieved via a simple one-step reaction. The size of the core and the thickness of the shell could be tuned by controlling parameters such as the concentration and temperature (Figure 4).

Depending on the initial shape of the cores, the carbon–noble metal nanostructures can be tuned from core–shell nanoparticles to nanocable structures.[26] During the synthesis of Ag@C nanocables, polygonal nanocrystals formed as nuclei, which grew along the $<01\bar{1}>$ direction because of the selective adsorption of PVP on specific crystal faces.[31] Carbonization of glucose took place at 180 °C (step 1 in Figure 3a). As-formed carbonaceous growth units stuck preferentially on the edges of polygonal crystals since these sites had higher surface tension and more dangling bonds. The adsorption inhibited the growth of convex edges. During the following growth process, such adsorption inhibited edge formation and finally resulted in a circular cross section (step 2). However, as the hydrothermal temperature was reduced to 140 °C, the carbonization process was significantly delayed, and PVP-assisted growth led to well-crystallized pentagonal nanowires. The plasmon resonance spectrum of the polygonal nanocable was different from that of the cylindrical nanocables,[26] which was in agreement with the predictions of the theoretical models for silver nanowires with different cross-sectional symmetry and of nanowires with dielectric coatings.[32]

Besides Ag and other noble metal nanoparticles such as Au, this one-step encapsulation reaction can be applied to other systems such as oxides, chalcogenides, and nitrides for the formation of hybrid core–shell structures and makes it possible to integrate different nanocrystals into dielectric coatings.

Formation of Hollow Oxide or Nitride Microspheres with Carbonaceous Spheres as Templates. Besides their amazing encapsulation abilities in forming various carbon–metal core–shell nanostructures, these carbonaceous microspheres have been evidenced as effective hard templates in producing uniform oxides or nitride hollow microspheres,[27–30] because of their uniform sizes and outer reactive surface. As mentioned above, there is no need to perform an additional surface modification process when using these carbonaceous microspheres as templates because of their affluent functional groups.

The strategy used to obtain monodispersed hollow oxides and nitrides spheres could be described as follows (Figure 3c): (1) the adsorption of metal ions from solution into a surface layer, (2) calcination of the composite spheres in air to remove the carbon core, which results in oxide hollow spheres, and (3) in situ conversion of the as-prepared oxide hollow spheres into nitride hollow spheres in an ammonia atmosphere at 700–900 °C. The surface of the carbonaceous spheres was hydrophilic, being functionalized with OH and C═O groups according to IR, Raman, and EDS studies.[27] Upon dispersal of the carbonaceous microspheres in metal salt solutions, the functional groups in the surface layer were able to bind metal cations through coordination or electrostatic interactions. This step would create solid–solid microinterfaces between carbon and metal species. In the subsequent calcination process, the surface layers incorporated with the cationic metal ions were densified and cross-linked to form oxide hollow spheres with a reduced size (~40% of the original, Figure 5). Since the interaction between the metal ions and the functional groups like OH is quite general, it is demonstrated that this is a general method for obtaining oxide or nitride hollow spheres using the common cationic forms of main group metals (Al^{3+}, Ga^{3+}, and Sn^{4+}), transitional metals (Mn^{2+}, Ni^{2+}, Cr^{3+}, Co^{2+}, Ti^{4+}, and Zr^{4+}), and rare-earth metals (La^{3+}, Y^{3+}, Lu^{3+}, and Ce^{3+}).

Recently, this strategy has been further modified as a one-pot hydrothermal approach, in which the preparation of carbonaceous microspheres and the incorporation of metal ions into the spheres were achieved simultaneously.[35] Both processes were based on the initial formation of solid–solid interfaces, which represent a generalized synthesis of metal oxide hollow spheres and can contribute to further development in the field.

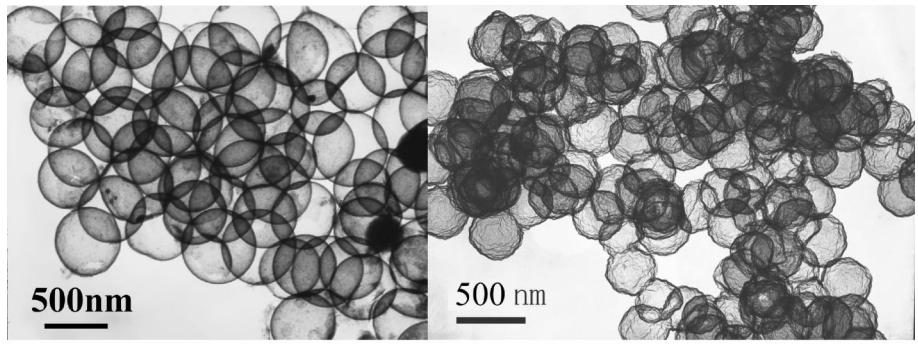

FIGURE 5. Typical TEM images of Ga_2O_3 hollow spheres prepared by using carbonaceous spheres as templates. (a) Carbonaceous microspheres were obtained from glucose solutions. (b) Carbonaceous microspheres were obtained from sucrose.

4. Liquid–Solid–Solution Phase Transfer and Separation Strategy and Oil–Water Interface-Controlled Reaction to Monodispersed Nanocrystals

Liquid–Solid–Solution Phase Transfer and Separation Strategy. The first two parts of this Account summarize our recent endeavor on the synthesis of hollow or core–shell nanostructures via surface-mediated approaches. It is worth noting that all of these reactions take place mainly in an aqueous system. While these synthetic routes are relatively environment-friendly and the as-obtained nanostructures are rather uniform in size, these aqueous-based routes are only suitable for nanostructures with sizes greater than 100 nm. The main reasons may be due to the surface-induced agglomeration of nanocrystals with diameters of <10 nm. The aggregation of the nanocrystals was avoided in an organic solvent-based synthetic route via the adsorption of surfactants onto the surfaces of the nanocrystals.[9–12] However, in an aqueous-based synthetic route, organic surfactants with long alkyl chains are usually insoluble in water so that the aqueous systems are only stable for nanocrystal aggregates or nanocrystals with larger diameters.

We have developed a liquid–solid–solution phase transfer and separation strategy to partially meet this challenge by carefully designing the chemical reactions taking place at the interfaces of different phases.[34] In this approach, a water/ethanol mixed solution is used as the main continuous solution phase. Since water is an ideal solvent for most inorganic species, and ethanol is a good solvent for most of the surfactants, including fatty acid, most of the soluble inorganic salts can be used as the starting materials. Long chain alkyl surfactants like octadecylamine or oleic acid can be used as protecting reagents for the nanocrystals. With these important features, this approach has been proven to be quite general in generating a huge group of monodispersed nanocrystals with sizes in the range of 2–15 nm, which have quite different crystal structures, compositions, and properties.[34–42]

With noble metal nanocrystals (such as Ag, Pd, Au, etc.) as examples, the primary reaction in the preparation of noble metal nanocrystals via this LSS process involved the reduction of noble metal ions by ethanol at the interfaces

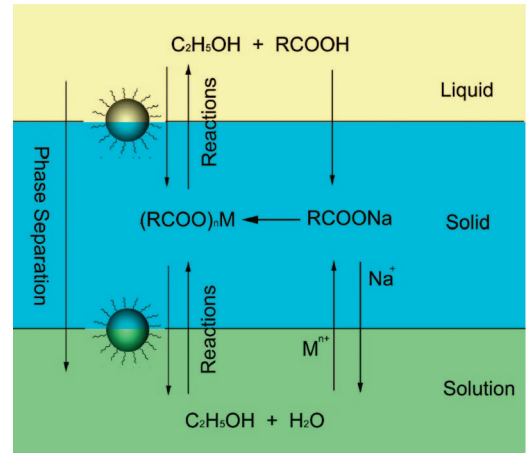

FIGURE 6. Liquid–solid–solution (LSS) phase transfer and separation synthetic strategy.

of metal linoleate (solid), an ethanol/linoleic acid liquid phase (liquid), and water/ethanol solutions (solution) at different designated temperatures (Figure 6). After aqueous solutions of noble metal ions, sodium linoleate (or other sodium stearate), and the mixture of linoleic acid (or other fatty acid) and ethanol were added into the vessel in that order, three phases would form in this system: sodium linoleate (solid), the liquid phase of ethanol and linoleic acid (liquid), and the water/ethanol solution containing noble metal ions (solution). A phase transfer process of the noble metal ions would occur spontaneously across the interface of sodium linoleate (solid) and the water/ethanol solution (solution) on the basis of ion exchange, which led to the formation of noble metal linoleate and the entering of the sodium ions into the aqueous phases. Then at a designated temperature, ethanol in the liquid and solution phases could reduce the noble metal ions at the liquid–solid or solution–solid interfaces. Along with the reduction process, the linoleic acid generated in situ would be absorbed on the surface of the noble metal nanocrystals with the alkyl chains left outside, through which the metal nanocrystals formed would be endowed with hydrophobic surfaces. Then a spontaneous phase separation process would occur because of the gravity of the metal nanocrystals and the incompatibility between the hydrophobic surfaces and

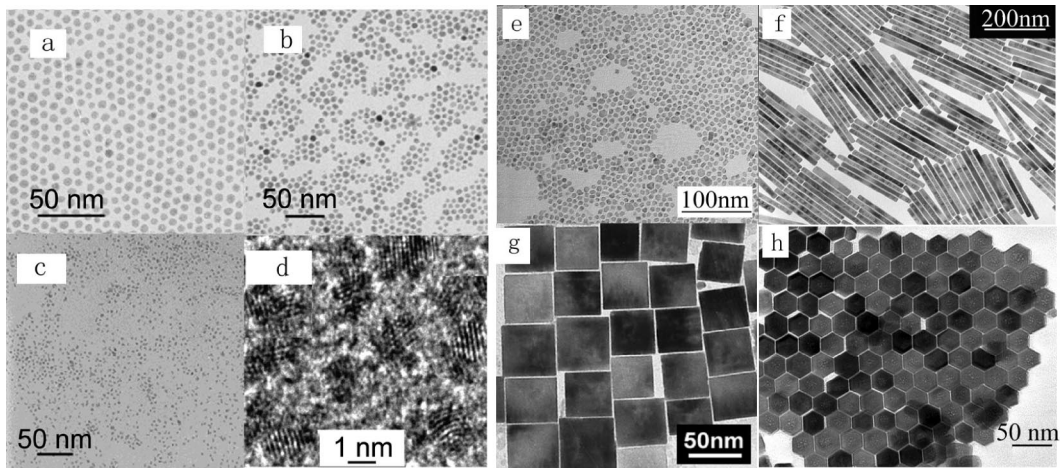

FIGURE 7. TEM images of nanocrystals with nearly round shapes synthesized via the LSS strategy: (a) Ag (6.1 ± 0.3 nm, 90 °C), (b) Au (7.1 ± 0.5 nm, 50 °C), (c) Rh (2.2 ± 0.1 nm, 120 °C), and (d) Ir (1.7 ± 0.09 nm, 120 °C). TEM images of nanocrystals with different shapes synthesized via the LSS strategy: (e) $NaYF_4$ nanoparticles, (f) $NaYF_4$ nanorods, (g) $LaVO_4$ nanocrystals with a square shape, and (h) $YPO_4 \cdot 0.8H_2O$ nanocrystals with a hexagonal shape.

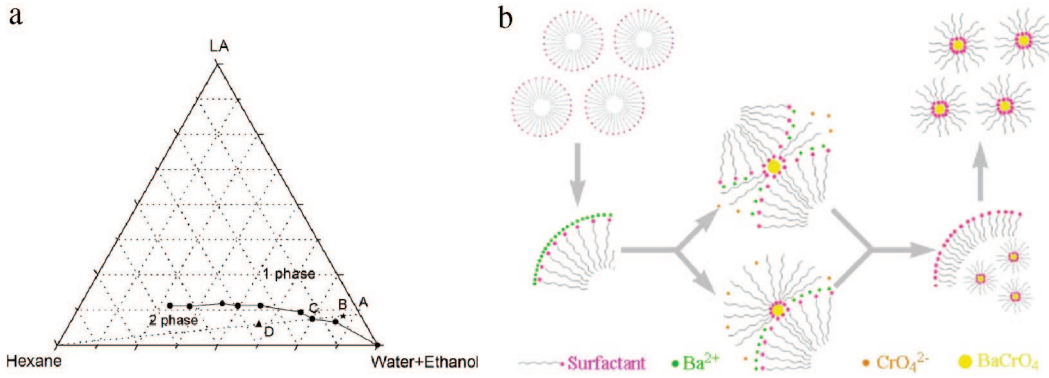

FIGURE 8. (a) Empirical phase diagram of the H_2O/EtOH/NaLA/LA/hexane microemulsions. (b) Proposed mechanism for the synthesis of colloidal nanoparticles via an oil–water interface-controlled reaction in normal microemulsions.

their hydrophilic surrounding, and the noble metal nanocrystals could be easily collected at the bottom of the container (Figure 7).

This LSS phase transfer and separation process has shown its amazing ability in generating various functional nanocrystals, including semiconductors, fluorescent, magnetic, and dielectric nanocrystals, etc.[34–42] The phase transfer process can occur for nearly all the transition or main group metal ions, which endows great flexibility for the reactions at the interfaces. After the phase transfer process that shifted the metal ions from the aqueous solution to the solid phase of $(RCOO)_nM$, under designed reaction conditions, the M^{n+} ions can dehydrate into oxides (to yield TiO_2, CuO, ZrO_2, SnO_2, ZnO, etc.) and/or composite oxides [to yield MFe_2O_4 (M = Fe, Co, Mg, Zn, Mn, etc.) and $MTiO_3$ (M = Ba or Sr) via coprecipitation)] or react with other anion species such as S^{2-} [S^{2-} was supplied by Na_2S or $(NH_4)_2S$, to yield CdS, MnS, PbS, Ag_2S, CuS, ZnS, etc.], Se^{2-} (Se^{2-} was generated by the reduction of SeO_3^{2-} by N_2H_4, to yield CdSe, ZnSe, etc.), or F^- (F^- was provided from NaF or NH_4F, to yield YF_3, LaF_3, $NaYF_4$, etc.) to yield various functional nanocrystals.

Besides the preparations of the uniform and nearly round-shaped nanocrystals, this LSS approach has shown its potential in controlling the shape of the as-obtained nanocrystals (Figure 7e–h). For example, when the temperature or concentration conditions were altered, apatite nanorods with different lengths were obtained,[35] and if the doping concentration of Ln^{3+} ions or the Y^{3+}/F^- ratio is controlled, the shape and size of luminescent $NaYF_4$ can be rationally controlled (Figure 7e,f).[39] Covered with long alky chains, these nanocrystals can self-assemble into ordered arrays via the interaction between the surfactants (Figure 7g,h).[41,42]

An Oil–Water Interface-Controlled Reaction in Normal Microemulsions for Preparation of Uniform Nanocrystals. Inspired by the special interface activity in the LSS strategy, an oil–water interface-controlled reaction in normal microemulsions (water/surfactant/hexane) was then applied to produce dispersive colloidal nanocrystals under ambient conditions (room temperature for most of the nanoparticles).[43,44] This method was based on the study of the phase behavior of the system. Figure 8a shows the empirical phase diagram for the water/ethanol/sodium linoleate (NaLA)/linoleic acid (LA)/hexane mixtures at room temperature (293 K). According to the phase diagram measurement, it can be concluded that with an increase in the LA/(H_2O + EtOH) ratio, more hexane can be dissolved into their mixtures to form a thermostable system. Because we were focusing on the oil-in-water

Table 1. Summary of the Source Materials, K_{sp} Values, Sizes, and Crystallinities for All Products Obtained via an Oil–Water Interface-Controlled Reaction

compound	source materials		K_{sp}	size (nm)	crystallinity
CdS	$Cd(NO_3)_2$[a]	Na_2S[a]	8.0×10^{-27}	2.0–4.0	poorly crystalline
ZnS	$Zn(NO_3)_2$[a]	Na_2S[a]	2.5×10^{-22}	2.5–4.5	poorly crystalline
Ag_2S	$AgNO_3$[b]	Na_2S[a]	6.3×10^{-50}	9.0–13.0	crystalline
PbS	$PbAc_2$[a]	Na_2S[a]	1.3×10^{-28}	2.5–3.0	crystalline
CdSe	$Cd(NO_3)_2$[a]	Na_2SeSO_3[a]	6.3×10^{-36}	2.0–3.0	poorly crystalline
Ag_2Se	$AgNO_3$[b]	Na_2SeSO_3[a]	2.0×10^{-64}	8.0–10.0	crystalline
PbSe	$PbAc_2$[a]	Na_2SeSO_3[a]	7.9×10^{-43}	4.0–6.0	crystalline
CaF_2	$CaCl_2$[a]	NaF[b]	2.7×10^{-11}	2.0–3.0	amorphous
YF_3	$Y(NO_3)_3$[a]	NaF[c]	6.6×10^{-13}	3.0–4.0	amorphous
PrF_3	$Pr(NO_3)_3$[a]	NaF[c]	7.1×10^{-17}	1.5–2.5	amorphous
NdF_3	$Nd(NO_3)_3$[a]	NaF[c]	–	1.5–2.0	amorphous
$HoPO_4$	$Ho(NO_3)_3$[a]	NaH_2PO_4[b]	–	2.0–3.0	amorphous
$CePO_4$	$Ce(NO_3)_3$[a]	NaH_2PO_4[b]	–	3.0–5.0	amorphous
$PbCrO_4$	$PhAc_2$[a]	K_2CrO_4[a]	2.8×10^{-13}	3.0–4.0	amorphous
$BaCrO_4$	$Ba(NO_3)_2$[a]	K_2CrO_4[a]	1.2×10^{-10}	2.0–4.0	amorphous
Ag	$AgNO_3$[a]	N_2H_4[d]	–	6.0–8.0	crystalline
Cu	$CuSO_4$[a]	N_2H_4[e]	–	2.0–3.0	crystalline

[a] Amount, 0.5 mmol. [b] Amount, 1.0 mmol. [c] Amount, 1.5 mmol. [d] At 80%, 1.0 mL. [e] At 80%, 3 mL.

microemulsion, more attention was paid to the bottom right region. The actual point we used is marked (point B) in the phase diagram and is located in the normal microemulsion region.

A mechanism based on the "interface-controlled reaction" was proposed to describe the formation of all of the nanoparticles (Figure 8b) as follows:[43] First, the transparent oil-in-water normal microemulsion forms after all the components are added according to the designed volume ratio. When metal cations such as Ba^{2+} were added to the solution, they were absorbed around the oil core due to the Coulomb attraction between Ba^{2+} and LA^-. Because the ions also had strong solvation properties in polar solvents, they would prefer to stay at the oil–water (O–W) interface so that they could be stabilized by both the polar solvent and the surfactant molecules. However, the injection of anions such as CrO_4^{2-} would destroy this balance by the "interface reaction" with Ba^{2+}. Considering the low solubility of these inorganic compounds, the original cations would quickly combine with the anions to produce small particles at the O–W interface. As the major phase in a normal microemulsion was water and ethanol, the whole process would be as fast as that in the common aqueous solutions. In most cases, the precipitation occurred within seconds. Since the particles that formed had a neutral electric charge, they were not as stable as the original cations at the interface. Because the particles were capped with surfactant, it is reasonable to predict a "phase transfer"; that is, the particles moved from the O–W interface to the inner oil core. Following this, the normal micelles recovered because of the supply of certain surfactant molecules free in the water phase, making them ready for the next interface reaction. The dynamic "reaction transfer" process happened alternatively and frequently, inducing the production of nanoparticles in a large amount and at a fast rate. Finally, hexane was added to destroy the single-phase status of the system, which is illustrated in the phase diagram (Figure 8a, point B to point D). The products extracted from the upper organic phase were washed with ethanol and redispersed in a nonpolar solvent. To improve the crystallinity of the nanocrystals, a hot liquid annealing process was adopted, during which the amorphous particles in the oil core were reorganized and crystallized to give larger particles due to Ostwald ripening. The shape and size may also be controlled by the confinement of micelles, which is similar to the situation in reverse microemulsions.

It is apparent that the current LSS and oil–water interface-controlled reaction strategies are superior to the reported synthetic methods in general, which provide us a general understanding on the formation mechanism concerning the interface-mediated growth. More studies are still needed to improve these strategies for precisely controlling the shape, size, and surface properties of the nanocrystals. Nevertheless, these advances in general synthesis led to progress in understanding the intrinsic size-dependent properties in different systems of nanocrystal building blocks and encourage some more unique and exciting applications from the bottom-up approach with these functional building blocks to nanotechnology for the subsequent research and application.[45,46]

Conclusion and Outlook. Nanoscience and nanotechnology still face the problem of manipulating nanoobjects at will. Interfaces as the transporting pathway for ion or atom species might be the most influential factors that deserve intense research attention in the process of fully addressing this problem. Despite all the success that has been achieved, more precise control over the dynamic process across the interfaces remains a challenging task, which may serve as the basis for the establishment of nanocrystal crystallography. Meanwhile, integration of monodispersed nanostructures into complex devices or superstructures is another problem that researchers face in nanoscience fields. The chemical and physical properties of surfaces and interfaces in nanocrystals are still the first issue to consider in the development of integration strategies.

We thank Prof. Joseph Chiang (State University of New York College at Oneonta, Oneonta, NY) for the polish of the English in the manuscript and helpful discussion. This work was supported by NSFC (90606006), the Foundation for the Author of National

Excellent Doctoral Dissertation of China, and the State Key Project of Fundamental Research for Nanoscience and Nanotechnology (2006CB932300).

References

(1) Eisenthal, K. B. Liquid Interfaces. *Acc. Chem. Res.* **1993**, *26*, 636–643.
(2) Rao, C. N. R.; Thomas, J. M. Intergrowth Structures: The Chemistry of Solid-Solid Interfaces. *Acc. Chem. Res.* **1985**, *18*, 113–119.
(3) Xia, Y. N.; Yang, P. D. One-Dimensional Nanostructures: Synthesis, Characterization, and Applications. *Adv. Mater.* **2003**, *15*, 353–389.
(4) Morales, A. M.; Lieber, C. M. A Laser Ablation Method for the Synthesis of Crystalline Semiconductor Nanowires. *Science* **1998**, *279*, 208–211.
(5) Duan, X. F.; Lieber, C. M. General Synthesis of Compound Semiconductor Nanowires. *Adv. Mater.* **2000**, *12*, 298–302.
(6) Wu, Y. Y.; Yang, P. D. Direct Observation of Vapor-Liquid-Solid Nanowire Growth. *J. Am. Chem. Soc.* **2001**, *123*, 3165–3166.
(7) Huang, M. H.; Wu, Y. Y.; Feick, H.; Tran, N.; Weber, E.; Yang, P. D. Catalytic Growth of Zinc Oxide Nanowires by Vapor Transport. *Adv. Mater.* **2001**, *13*, 113–116.
(8) Hu, J. T.; Odom, T. W.; Lieber, C. M. Chemistry and Physics in One Dimension: Synthesis and Properties of Nanowires and Nanotubes. *Acc. Chem. Res.* **1999**, *32*, 435–445.
(9) Yin, Y.; Alivisatos, A. P. Colloidal Nanocrystal Synthesis and the Organic-Inorganic Interface. *Nature* **2005**, *437*, 664–670.
(10) Trentler, T. J.; Hickman, K. M.; Goel, S. C.; Viano, A. M.; Gibbons, P. C.; Buhro, W. E. Solution-Liquid-Solid Growth of Crystalline III-V Semiconductors: An Analogy to Vapor-Liquid-Solid Growth. *Science* **1995**, *270*, 1791–1794.
(11) Murray, C. B.; Norris, D. J.; Bawendi, M. G. Synthesis and characterization of nearly monodisperse CdE (E = sulfur, selenium, tellurium) semiconductor nanocrystallites. *J. Am. Chem. Soc.* **1993**, *115*, 8706–8715.
(12) Sun, S. H.; Murray, C. B.; Weller, D.; Folks, L.; Moser, A. Monodisperse FePt nanoparticles and ferromagnetic FePt nanocrystal superlattices. *Science* **2000**, *287*, 1989–1992.
(13) Sun, Y. G.; Xia, Y. N. Shape-controlled synthesis of gold and silver nanoparticles. *Science* **2002**, *298*, 2176–2179.
(14) Mann, S.; Ozin, G. A. Synthesis of inorganic materials with complex form. *Nature* **1996**, *382*, 313–318.
(15) Yang, H.; Coombs, N.; Sokolov, I.; Ozin, G. A. Free-Standing and Oriented Mesoporous Silica Films Grown at the Air-Water Interface. *Nature* **1996**, *381*, 589–592.
(16) Yang, P. D. Wires on Water. *Nature* **2003**, *425*, 243–244.
(17) Peng, Q.; Dong, Y. J.; Li, Y. D. ZnSe Semiconductor Hollow Spheres. *Angew. Chem., Int. Ed.* **2003**, *42*, 3027–3030.
(18) Caruso, F. Hollow Capsule Processing through Colloidal Templating and Self-Assembly. *Chem.—Eur. J.* **2000**, *6*, 413–419.
(19) Caruso, F.; Caruso, R. A.; Mohwald, H. Nanoengineering of Inorganic and Hybrid Hollow Spheres by Colloidal Templating. *Science* **1998**, *282*, 1111–1114.
(20) Velikov, K. P.; van Blaaderen, A. Synthesis and Characterization of Monodisperse Core-Shell Colloidal Spheres of Zinc Sulfide and Silica. *Langmuir* **2001**, *17*, 4779–4786.
(21) He, R. R.; Law, M.; Fan, R.; Kim, F.; Yang, P. D. Functional Bimorph Composite Nanotapes. *Nano Lett.* **2002**, *2*, 1109–1112.
(22) Peng, Q.; Dong, Y. J.; Deng, Z. X.; Li, Y. D. Selective Synthesis and Characterization of CdSe Nanorods and Fractal Nanocrystals. *Inorg. Chem.* **2002**, *41*, 5249–5254.
(23) Peng, Q.; Xu, S.; Zhuang, Z. B.; Wang, X.; Li, Y. D. A General Chemical Conversion Method to Various Smiconductor Hollow Structures. *Small* **2005**, *1*, 216–221.
(24) Sun, X. M.; Li, Y. D. Colloidal Carbon Spheres and Their Core/shell Structures with Noble-Metal Nanoparticles. *Angew. Chem., Int. Ed.* **2004**, *43*, 597–601.
(25) Sun, X. M.; Li, Y. D. Ag@C Core/shell Structured Nanoparticles: Controlled Synthesis, Characterization and Assembly. *Langmuir* **2005**, *21*, 6019–6024.
(26) Sun, X. M.; Li, Y. D. Cylindrical Silver Nanowires: Preparation, Structure and Optical Properties. *Adv. Mater.* **2005**, *17*, 2626–2630.
(27) Sun, X. M.; Li, Y. D. Ga_2O_3 and GaN Semiconductor Hollow Spheres. *Angew. Chem., Int. Ed.* **2004**, *43*, 3827–3831.
(28) Sun, X. M.; Liu, J. F.; Li, Y. D. Use of Carbonaceous Polysaccharide Microspheres as Template for Fabricating Metal Oxide Hollow Spheres. *Chem.—Eur. J.* **2006**, *12*, 2039–2047.
(29) Sun, X. M.; Liu, J. F.; Li, Y. D. Oxides@C Core-Shell Nanostructures: One-Pot Synthesis, Rational Conversion and Li Storage Property. *Chem. Mater.* **2006**, *18*, 3486–3494.
(30) Li, X. L.; Lou, T. J.; Sun, X. M.; Li, Y. D. Highly Sensitive WO_3 Hollow-Sphere Gas Sensors. *Inorg. Chem.* **2004**, *43*, 5442–5449.
(31) Wiley, B.; Sun, Y. G.; Mayers, B.; Xia, Y. N. Shape-controlled Synthesis of Metal Nanostructures: The Case of Silver. *Chem.—Eur. J.* **2005**, *11*, 454–463.
(32) Kottmann, J. P.; Martin, O. J. F.; Smith, D. R.; Schultz, S. Plasmon Resonances of Silver Nanowires with a Nonregular Cross Section. *Phys. Rev. B* **2001**, *64*, 235402.
(33) Titirici, M. M.; Antonoetti, M.; Thomas, A. A Generalized Synthesis of Metal Oxide Hollow Spheres Using A Hydrothermal Approach. *Chem. Mater.* **2006**, *18*, 3808–3812.
(34) Wang, X.; Zhuang, J.; Peng, Q.; Li, Y. D. A General Strategy for Nanocrystal Synthesis. *Nature* **2005**, *437*, 121–124.
(35) Wang, X.; Zhuang, J.; Peng, Q.; Li, Y. D. Liquid-Solid-Solution Synthesis of Biomedical Hydroxyapatite Nanorods. *Adv. Mater.* **2006**, *18*, 2031–2034.
(36) Wang, X.; Zhuang, J.; Peng, Q.; Li, Y. D. Hydrothermal Synthesis of Rare Earth Fluoride Nanocrystals. *Inorg. Chem.* **2006**, *45*, 6661–6665.
(37) Wang, X.; Zhuang, J.; Peng, Q.; Li, Y. D. Synthesis and Characterization of Sulfide and Selenide Colloidal Semiconductor Nanocrystals. *Langmuir* **2006**, *22*, 7364–7368.
(38) Liang, X.; Wang, X.; Zhuang, J.; Cheng, Y. T.; Wang, D. S.; Li, Y. D. Synthesis of Nearly Monodisperse Iron Oxide and Oxyhydroxide Nanocrystals. *Adv. Funct. Mater.* **2006**, *16*, 1805–1813.
(39) Wang, L. Y.; Li, Y. D. $Na(Y_{1.5}Na_{0.5})F_6$ Single Crystal Nanorods as Multicolor Luminescent Materials. *Nano Lett.* **2006**, *6*, 1645–1649.
(40) Ge, J. P.; Xu, S.; Zhuang, J.; Wang, X.; Peng, Q.; Li, Y. D. Synthesis of CdSe, ZnSe, and $Zn_xCd_{1-x}Se$ Nanocrystals and Their Silica Sheather Core/Shell Structures. *Inorg. Chem.* **2006**, *45*, 4922–4927.
(41) Liu, J. F.; Yao, Q. H.; Li, Y. D. Effects of Downconversion Luminescent Film in Dye-Sensitized Solar Cell. *Appl. Phys. Lett.* **2006**, *88*, 173119.
(42) Huo, Z. Y.; Chen, C.; Li, Y. D. Self-Assembly of Uniform Hexagonal Yttrium Phosphate Nanocrystals. *Chem. Commun.* **2006**, 3522–3524.
(43) Ge, J. P.; Chen, W.; Liu, L. P.; Li, Y. D. Formation of Disperse Nanoparticles at the Oil/Water Interface in Normal Microemulsions. *Chem.—Eur. J.* **2006**, *12*, 6552–6558.
(44) Ge, J. P.; Xu, S.; Liu, L. P.; Li, Y. D. A Positive-Microemulsion Method for Prepaing Nearly Uniform Ag_2Se Nanoparticles at Low Temperature. *Chem.—Eur. J.* **2006**, *12*, 3672–3677.
(45) Burda, C.; Chen, X. B.; Narayanan, R.; El-Sayed, M. A. Chemistry and Properties of Nanocrystals of Different Shapes. *Chem. Rev.* **2005**, *105*, 1025–1102.
(46) Phillips, J. M. Nanoscale Science Research Centers. *MRS Bull.* **2006**, *31*, 44–49.

AR600007Y